Field correlation between shear wave velocity measured by Panda 3®, cone penetration test (CPT) and geophysical tests

A. Teyssier
Fondasol, Avignon, France, alexandre.teyssier@fondasol.fr

M.A. Benz Navarrete[1], Q. Anh Tran[2], J.C. Pellez[3]
Sol Solution, Riom, France, mbenz@sol-solution.com[1], qatran@sol-solution.com[2], jcpellez@sol-solution.com[3]

C. Jacquard[1]
Fondasol, Avignon, France, catherine.jacquard@fondasol.fr [1]

ABSTRACT: This paper will present a field comparative study between shear wave velocity measurements (V_s), deduced from compression wave velocity (V_p) and signal analysis with Panda 3® test, and those obtained by correlation through CPT tests and seismic surface wave method (MASW) on a sandy site in southern of France. The purpose of this paper is to confirm the consistency of Panda 3® shear wave measurements with measures resulting from traditional geotechnical investigation methods.

Keywords: Shear wave velocity; Panda®; Cone penetration test; Ménard pressuremeter test; geophysical tests.

1. Introduction

The soil shear wave velocity (V_s) is one of the key parameters in studying soil behaviour under seismic stresses (earthquakes). Shear waves are waves whose movement is perpendicular to the direction of propagation of the wave and they do not spread in liquids. Shear wave velocity varies according to the environments crossed, especially according to their density.

Thus, the measurement of shear wave velocity is today the reference parameter for the classification of soils under seismic stresses in many countries and used for the study of the risk of liquefaction on buildings.

1.1. Geophysical investigations

Currently, in the field practice shear wave velocity V_s is mainly measured by geophysical methods: Crosshole/Downhole, MASW, H/V method as well as correlated with sCPT, sDMT, sPMT…

The most commonly used methods are Crosshole/Downhole (ASTM D 4428/D5528 M [1]). These are also the recommended methods in most of the worldwide standards (Europe, United States, Japan, Canada, etc.) in order to determine the shear wave velocity in soils. These methods measure compressional and/or shear wave propagation, either between two/three boreholes (Crosshole) or between a borehole and a receiving source usually placed on the surface (Downhole).

These techniques allow a measurement of the shear wave velocity for each recorded blow at different depth, i.e. one measurement every meter or so. Its requires one to three preliminary boreholes to be drilled using a drilling technique that disturbs as little as possible the surrounding soil. These must be equipped with a sealed borehole pipe. The seal to be used must have a limited impact on the wave propagation.

On the other hand, the MASW (Multichannel Analysis of Surface Waves) method is based on the analysis of surface waves, and more particularly Rayleigh waves, generated by a surface point source (active source). This method, increasingly used, is described by C. B. Park and al [2] and makes it possible to characterize the soil in terms of shear wave velocity over a fairly limited depth.

1.2. Geotechnical shear wave correlation

In the absence of Crosshole/Downhole tests, correlations based on geotechnical test such as cone penetration test (CPT) or Ménard pressuremeter test (PMT), are often used. These relationships make it possible to obtain correlated values of shear wave velocity that can be used to carry out a soil seismic classification or to assess the risk to liquefaction phenomenon. Their application often has a limited and specific scope. Some correlations give a shear wave velocity (V_s) directly, others give access to the shear modulus (G), linked to the velocity by the following relationship Eq. (1):

$$G = \rho \, . \, V_s^2 \quad (1)$$

With: ρ: density

Some examples of correlations [3]–[8] can be given:

- For clays, Mayne ([4], [5]) Eq. (2) :

$$G_{max} = 406(q_c)^{0.695}e^{-1.13} \quad (2)$$

- For sands, Jamiolkowski [7] Eq. (3) and Robertson [9] Eq. (4) :

$$G_{max} = 1634(q_c)^{0.259}(\sigma'_v)^{0.375} \quad (3)$$

$$V_S = \sqrt{\frac{10^{(0,55I_c+1,68)}(q_t-\sigma_v)}{p_a}} \quad (4)$$

1.3. Shear wave velocity measurement applications

For the seismic classification of a site, it is necessary to carry out investigations to assess the shear wave velocity over at least 30 meters of depth [10], [11] [12]. It is thus possible to calculate the parameter $Vs_{,30}$ according to the following relationship Eq. (5) :

$$V_{s,30} = \frac{30}{\sum_1^N \frac{h_i}{v_i}} \quad (5)$$

With: h_i: thickness of the i^{th} layer on a total of existing N over the upper 30 meters.

v_i : shear wave velocity of the i^{th} layer over a total of N existing over the upper 30 meters.

In addition, for the assessment of soil liquefaction susceptibility through shear wave velocity measurements, one of the main methods used is presented by B. R. D. Andrus [13]. The liquefaction potential is evaluated by a safety factor FS which is calculated according to the following Eq. (6):

$$FS = \frac{CRR}{CSR} \quad (6)$$

With CRR: Cyclic Resistance Ratio (ratio of stresses that the soil will resist and beyond which the shear strength is cancelled) and CSR: Cyclic Stress Ratio (earthquake-induced shear stress ratio).

1.4. Limitations

Most investigation methods can achieve the shear wave velocity at significant depths. However, surface soils present the most immediate risks for construction and are not sufficiently characterized in terms of shear wave velocity.

On the other hand, penetration tests and specially Panda penetrometer [14] have a particular interest to complete the shallow investigation program. In addition to being lightweight, easily transportable and applicable in many contexts, it allows a fine characterization on the first metres of ground. However, their first generations only provide dynamic cone resistance and it is therefore necessary to find ways to better explode the recorded signals in order to improve the results achieved with Panda.

2. Dynamic penetrometer Panda 3®

2.1. General measurement principle

Developed during the last ten years [15]–[17], the main principle of dynamic lightweight penetrometer Panda 3 (Fig. 1) is as follows: for each impact provided during penetrometer driving, changes of strain ε(t) and acceleration a(t) caused by compression wave are measured in the rod, near the anvil. In fact, when the hammer hits the anvil, a compression wave u(x,t) is created in the rods propagating at constant speed c_t towards the tip. When the wave $u(x,t)$ arrives at the tip/soil interface, part of it is used to penetrate the soil. The other part is reflected into the rods towards the surface. Return cycles within rods continue until the total energy of the waves is not sufficient to penetrate the soil. The propagation phenomenon of the wave $u(x,t)$ in the rods of a driven penetrometer is described by the wave equation [18], [19]. During its propagation, the wave $u(x,t)$ causes at any x point along the rods strain $\varepsilon(x,t)$ and velocity $v(x,t)$ changes represented by the superposition of the two elementary waves (downward u_f and u_g upward waves respectively).

One of the most commonly used solutions is that obtained by the characteristic method [20], [21], represented by the superposition of these two elementary waves, u_f and u_g; within an elastic and homogeneous medium.

If these waves are known at a given point on the rods, it is possible to evaluate at any x point along the rods stress, acceleration, velocity and displacement [22]. In addition and in the most general case where the rod is considered elastic, wave propagation can be explained from its Fourier components [23]. In the BCGO method [22] applied to the dynamic penetrometer, the stress $\sigma(x,t)$, strain $\varepsilon(x,t)$, velocity $v(x,t)$ as well as displacement $u(x,t)$ in a measurement point x along rods are expressed according to equations involving the Fourier $A(\omega)$ and $B(\omega)$ components of the downward and upward waves.

These are defined by $E^*(\omega)$ the complex Young's modulus and $\xi(\omega) = k(\omega)+i\alpha(\omega)$ the complex wave number. It can be noted that all the dynamic quantities can be obtained if the following values are known: $E^*(\omega)$, $\xi(\omega)$, $A(\omega)$ and $B(\omega)$.

Accepting that $E^*(\omega)$ and $\xi(\omega)$ are determined only by the geometric and material properties of the rods, wave decoupling therefore consists in determining the values of components $A(\omega)$ and $B(\omega)$.

2.2. Dynamic load-penetration curve

Wave reconstruction technique implemented in Panda 3 consists in calculating the force $F_N(t)$ and velocity $v_N(t)$ - according to equations given by Benz and al. (2013) [15], [16] - at each section with an impedance change along the rods and especially at the cone tip/soil interface [24]–[28]. In the time domain, force and velocity can be written as a fonction of recorded force and velocity in a measurement section along the rod.

Once the signals have been reconstructed and by making some simplifying assumptions, the load-penetration curve is plotted for each blow (Fig. 1). An analytical methodology, similar to that used for pile dynamic load test [29]–[31], has been implemented in order to establish different soil parameters : dynamic ($q_{d,w3}$) and pseudo-static ($q_{s,w3}$) cone resistance, reloading ($E_{r,w3}$) and unloading modulus ($E_{d,w3}$), compression ($v_{p,w3}$) and shear wave ($v_{s,w3}$) velocity as well as a damping coefficient ($J_{s,w3}$).

The total measured resistance $q_{d,w3}(t)$ – which is time-dependent – is the result of a pseudostatic component $q_{s,w3}(t)$ (which obeys an elastic-perfectly plastic law) and a dynamic component $R_d(t)$. This last one is proportional to the penetration velocity $v_p(t)$ as well as the soil mechanical impedance Z_s.

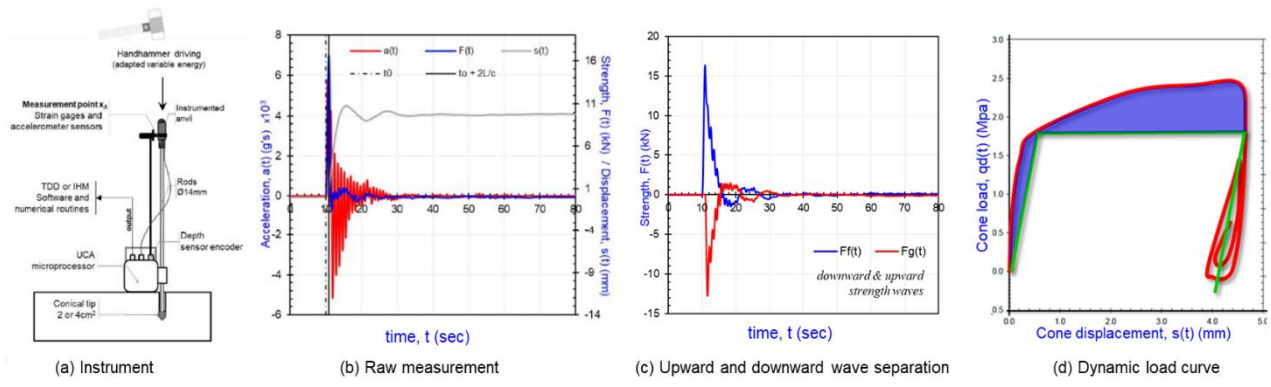

Figure 1. General principle of Panda 3® Test (a) Panda 3® device, (b) raw measurements, (c) wave decoupling and (d) Dynamic load/penetration curve obtained for each blow.

Pseudostatic resistance $q_{s,w3}$ are determined at the moment when the tip penetration velocity $v_p(t)$ equals zero. In this moment dynamic resistance $R_d(t)$ cancels itself and $q_{s,w3}$ is then equal to $q_{d,w3}(t)$.

Furthermore, once the maximum penetration (s_{max}) is reached, it is assumed that the soil and penetrometer vibrate together in a pseudo-elastic regime. In this part of load-penetration curve, two modulus are defined: an unloading modulus $E_{d,w3}$ (green line in Fig. 1.d) and a reloading modulus $E_{r,w3}$ (yellow line in Fig. 1.d). Assuming that the cone tip penetrometer can be similar to a small circular plate embedded in a semi-infinite elastic media, the value of $E_{r,w3}$ and $E_{d,w3}$ by means of Boussinesq equation as proposed by [32].

Some work has already been done on the application of this new technique in soil shallow characterization [33]–[35]. However, none of these studies addressed the subject of the comparison as well as its correlation with measurements of soil shear waves velocity made by the other methods.

2.3. Soil wave velocity by polar of shock

In order to determine the soil mechanical impedance, celerity as well as strain, the shock polar curve method [36]–[38] is applied as shown in Fig. 2. The polar shock curve represents the relationship between stress and particular velocity generated by the passage of a shock wave within the rods. In this method, it is assumed there is propagation of a plane and unidirectional elastic shock wave travelling in a medium A (the rods) to a medium B (the soil). Both media have different impedance values and in our case, that of the rods is greater than the soil. The main objective is to obtain the soil shock polar curve from decoupled strain waves recorded in the measurement section x_A on the penetrometer rods.

Considering the penetrometer and soil at rest, just after the hammer blow, the rods are crossed by the compression incident wave $u_f(t)$ and after its passage the relationship between stress σ_f and particular velocity v_f can be expressed (Eq. (6)). When the incident wave reaches the soil/tip interface, a transmitted wave $u_T(t)$ into the soil occurs while a reflected wave $u_g(t)$ is returned upwards into the rods to the top. The resulting stress after its passage can be expressed according to Eq. (7). The pair of points (σ_f, v_f) and (σ_g, v_g) belong to the rod's polar shock, defined by the slope $Z = \rho c$, where ρ is the density and c the wave velocity (celerity) of the steel rod.

$$\sigma_f = \frac{E}{c} v_f = \rho c v_f \tag{7}$$

$$\sigma_g = -\frac{E}{c} v_g = -\rho c v_g$$

In the soil, immediately after the passage of the transmitted wave $u_T(t)$, the stress σ_T and the particular velocity v_T increase proportionally, according Eq. (8). At the soil/tip interface the incident and reflected wave overlap and resulting stress and particular velocity can be expressed as a function of these waves according to Eq. (8). Thus, the point (σ_T, v_T) belongs to the soil's polar shock curve.

$$\sigma_T = \frac{E_s}{c_s} v_T = \rho_s c_s v_T \tag{8}$$
$$\sigma_T = \sigma_f - \sigma_g$$
$$v_T = v_f - v_g$$

In the case of steel (for the penetrometer rods), the polar shock curve is a straight line defined by the slope $Z = \rho c$; while for the soil, the shape of this curve remains unknown and must be determined experimentally.

In practice, a part of soil polar shock curve can be obtained from penetrometer measurements and for the time interval $t_0 + 2L/c$ as follows:

1. Consider decoupled incident, reflected waves.
2. Compute stress and velocity for incident and reflected waves.
3. Compute stress and velocity of transmitted wave at the tip of the penetrometer.
4. Plot transmitted stress as a function of transmitted velocity and fitting the curve $\sigma_T = Z_s v_T$.

Knowing the soil impedance Z_s, and considering that for the short duration of the analysis the soil behaviour is elastic and that it has no time to deform radially, it is possible to determine the compression soil wave velocity c_s, as well as the strain ratio, according to Eq. (9).

$$c_s = \frac{Z_s}{\rho_s} \tag{9}$$
$$\varepsilon_{xx} = \frac{v_T}{c_s}$$

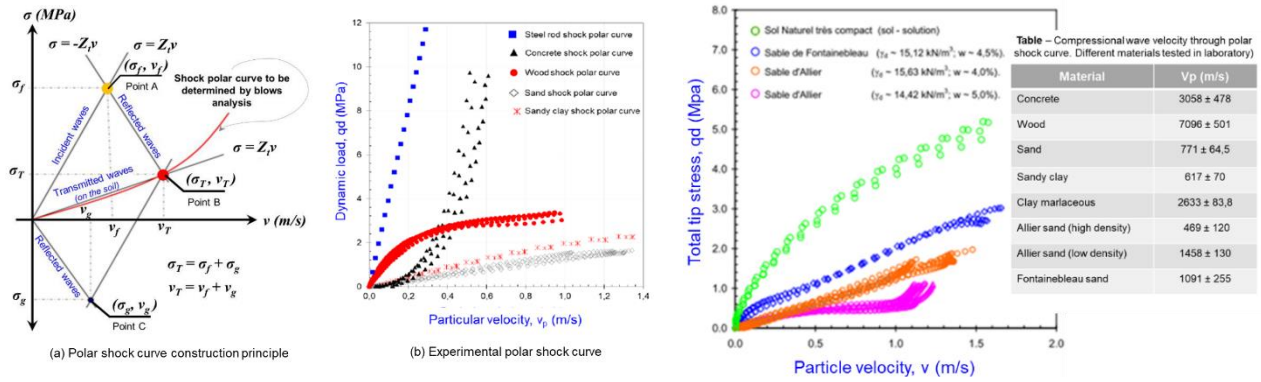

(a) (b)

Figure 2. Soil wave measurement principle with Panda 3® based on shock polar curves (Aussedat, 1970) [36] . (a) Polar construction principle adapted from Aussedat and experimental curves for steel, concrete, wood and loose sand and (b) Experimental shock polar curves obtained for different soils, at different density state in laboratory by Benz (2009)[15], [16]. In the graphs every curve represents one blow during penetrometer driving. Simultaneously, on the figure 2.b, a summary table of the results obtained in laboratory is also presented.

Recorded measurements carried out throughout the test, and decoupled waves are presented in Fig. 1 b-d. Reconstructed signals at the tip of the penetrometer (velocity, displacement and strength) by means of the present method are also presented.

Once the soil compression wave velocity is obtained, it is possible to calculate a shear wave velocity according to Eq. (10) [39], [40] and a Poisson coefficient ν :

$$V_s = V_p \sqrt{\frac{1-2\nu}{2(1-\nu)}} \qquad (10)$$

2.4. Previous comparative results

The main interest of a test such as the one proposed by the Panda 3®, is the fact that it is possible to characterize surface formations (z < 7m) quite finely, particularly with regard to the evaluation of the elastic properties of soils, such as wave celerity. In order to show the interest shown in this new auscultation technique and to validate the results obtained, various studies were carried out.

With regard to the evaluation of wave velocity using Panda 3®, as a first step, the feasibility and relevance of measuring compression wave velocities (V_p) using shock polarities in the laboratory is evaluated. To do so, the authors reproduced the experiments carried out by Aussedat in 1960 [36], but for different materials and using a penetrometer. The results obtained in Fig. 2b show the reliability of the technique and the good correspondence of the results obtained with those indicated in the literature.

Subsequent work was mainly devoted to the in-situ validation of such measurements; to this end, comparative tests were carried out at various experimental sites. The results obtained were mainly compared with the results obtained through the CPT, PMT, SPT, DPSH... in terms of soil resistance. With regard to the comparison of wave velocity measurements, the results were mainly compared with those obtained by surface seismic methods (MASW, Refraction).

In Fig. 3, a comparison of shear wave velocity results obtained at three sites, two in France and one in Spain (Castello d'Empuriés, close to Girona) is presented. These three sites have different geological formations. In addition, various geotechnical and geophysical tests were available to compare the results obtained.

In Fig. 3b, the results obtained at the Castelo d'Empuries site (Spain), we can observe the good correspondence for the first 6 meters of the soundings of the three techniques used: MASW2D, sDMT and Panda 3®. For the Zuytpeene site (a French commune in the Nord department in northern France, south of the Dunkirk city) in Fig. 3c, we compared not only the value of the shear wave velocities V_s but also the compression velocity V_p. On this site, composed mainly of Flanders Clay, refraction and MASW profiles were available.

In all cases the results obtained show that the measurements provided correspond well. It is also interesting to note, despite the fact that the Panda 3® signals presented in Fig. 3 are smoothed and standardized, that they have a much finer vertical resolution for the first few meters compared to the results obtained with the other methods.

This makes the Panda 3® technique very interesting for characterizing sites where access is difficult (tailing dams, foundations of vibrating machines, railways...) or on common sites where a high vertical and/or spatial resolution is required in order to characterize soils having a very low density and/or a very low bearing capacity.

Although there are many previous experiments and the results presented show a good correspondence with those obtained by means of geophysical methods, in most cases, the results presented were obtained on sites composed of fine soils with medium to high compaction.

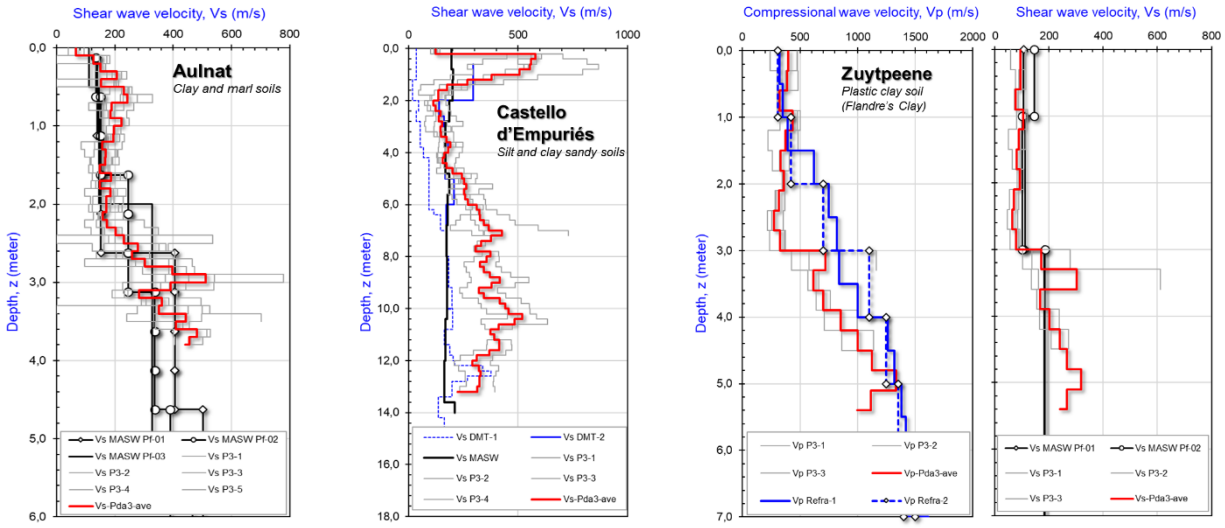

(a) (b) (c)

Figure 3. Soil's wave velocity determined by means Panda 3® test. Previous comparative results in three sites (a) Aulnat (French site, clay and marls soil profile), (b) Castello d'Empuriés in Girona Spain (deltaic site, with sandy, silty and clayey soils in depth. For this site, measurements made with SDMT are also compared) and (c) Zuytpeene (French site in the north) (data source: [41], [42] and Sol Solution internal database). For the case of Zuytpeene site, a comparison with the compression wave velocity determined by seismic refraction is presented.

3. Experimental campaign

In comparison with previous studies, an extensive Panda 3® investigation campaign was carried out on a site consisting of sandy embankments in the port of Sète (Hérault, south of France).

3.1. Site description

The Sète site is a land reclaimed from the sea in the summer of 2019. It was backfilled by dredging sand to a height of between 4 and 7 to 8 meters.

3.2. Test performance

At the Sète site, numerous investigations were carried out, as summarized in Fig. 4a:

- 2 core boreholes (SC) at a depth of 8 to 10 m
- 2 pressuremeter boreholes (SP), coupled with core boreholes, dropped to a depth of 26 m.
- 9 cone penetration tests (CPT) dropped to a depth of 4 to 9m.
- 4 piezocone penetration tests (CPTu) descended to a depth of 9 to 15m.
- 21 geological pits, 2.60 to 2.90m depth
- 4 MASW2D profiles
- 2 Passive seismic profiles (Remi), and
- 4 Refraction profiles

On each of these points, Fig. 4 b-c:

- 1 dynamic penetration test Panda 3® (11 tests in all at a final depth of 6 meters)
- 1 dynamic penetration test Panda (14 tests at a final depth of 6 meters), and
- 1 Grizzly-EV variable energy DPSH penetration test (11 tests at a final depth between 6 < z < 18 m).

These last test, Panda and Grizzly-EV, were drilled in order to multiply the measurements and to better evaluate the vertical heterogeneities of the embankment but also to establish the density profile of the sands composing the embankment.

3.3. Site results

Analysing the first 6 meters of both tests (in Fig. 5), we can see a good agreement of the obtained results for the shallow embankment in terms of resistance (p_{LM}, qc & q_d) with SP1, SP2 and CPT1 as well as modulus (E_M & E_{dp3}) obtained by mean PMT tests. The high vertical resolution of the Panda 3® measurements is again highlighted and in this particular case is a very good complement for Pressurementer test (PMT), especially in shallow depth.

From whole graphs presented in Fig. 5 it is possible to identify four main layers constituting the embankment (6 to 7 meters height):

- 1st medium compaction layer (0-1.80m),
- 2nd very loose sandy layer (1.80 to 4.60m)
- 3rd transition compact sand layer (4.60 to 6m)
- The bottom layer (z > 6m).

From piezocone penetration tests (CPTu) and geological pits, it is possible to determine the groundwater table depth around 2.40m. That depth can fluctuate depending on the distance from the shore and the level of the floor.

(a) (b) (c)

Figure 4. Experimental campaign carried out in a sandy soil embankment at Sète (France) (a) The site location and implementation of investigations on Sète site, (b) Panda 3® test carried out on the site and (c) seismic surface survey by means MASW2D technique

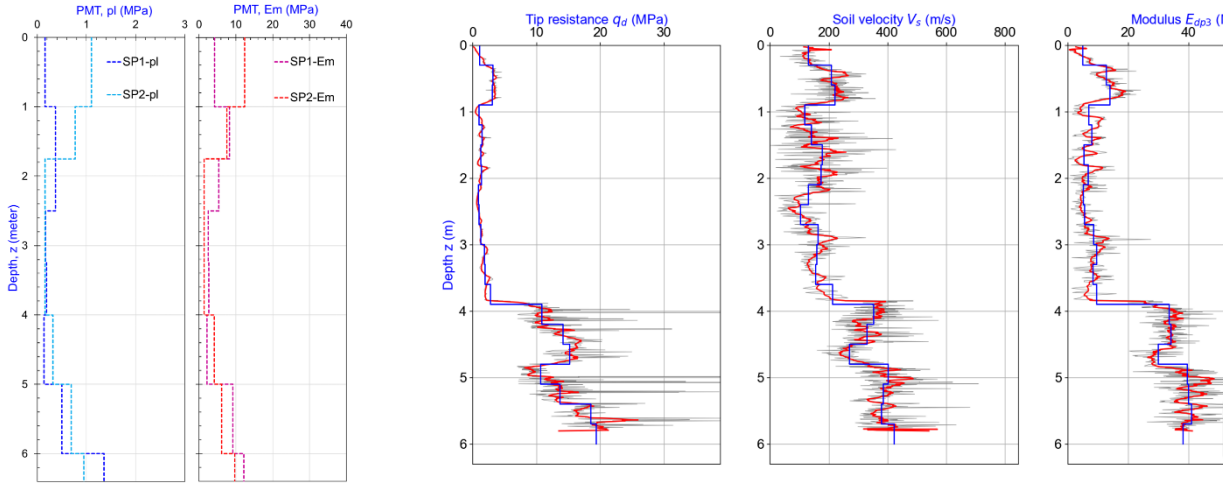

(a) (b)

Figure 5. Experimental campaign on Sète Site – Test results: (a) Pressuremeter results (SP1 & SP2) and (b) Example of Panda 3® test (Pda3-CPT1) results (raw (gray line), smoothed (red line) and regularized (blue line)).

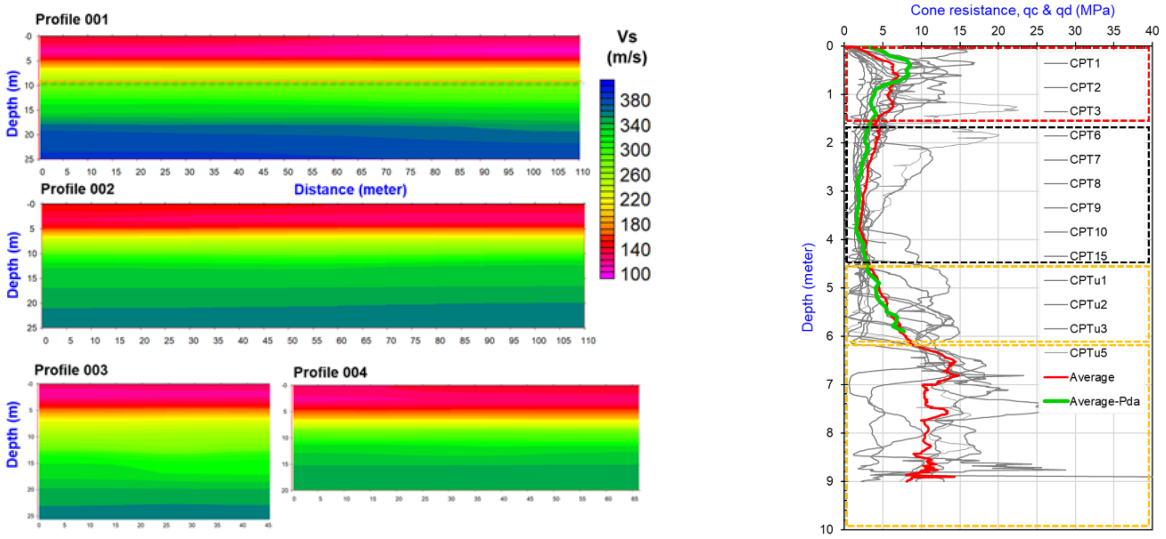

(a) (b)

Figure 6. Experimental campaign on Sète Site – test results (a) MASW2D obtained profiles and (b) All CPTs cone resistance (qc) recorded (grey line) as well as the average signal (red line).

Table 1. Experimental campaign on Sète Site – Summary of geotechnical results by means different test.

Average & (Stdv)		**Layer 1** (compact sandy soil)				**Layer 2** (loose sandy soil)				**Layer 3** (compact sand layer)		
Panda 3	1,80	**qd (MPa)**	**Vs (m/s)**	**E_{dp3} (MPa)**	4,60	**qd (MPa)**	**Vs (m/s)**	**E_{dp3} (Mpa)**	6,00	**qd (MPa)**	**Vs (m/s)**	**E_{dp3} (MPa)**
		5,97 (3,18)	222 (96,7)	19 (9,17)		2,86 (1,07)	168 (53,9)	12 (4,31)		12,48 (4,76)	365 (66,7)	36 (8,5)
Vs MASW (1D & 2D)	1,80	130 (13,8)			4,60	129 (11,4)			6,00	167 (48,4)		
E_M (MPa) - PMT	1,80	7,18 (3,51)			4,60	4,13 (2,37)			6,00	15,5 (14,3)		
P_{LM} (MPa) - PMT		0,47 (0,42)				0,21 (0,10)				0,35 (0,24)		
qc (MPa) - CPT	1,80	4,5 (3,2)			4,60	2,2 (2,0)			6,00	3,2 (4,0)		
Vs (m/s) - CPT		167 (24,9)				190 (5,1)				215 (8,1)		
Unit Weight (kN/m3)	1,80	17,1 (0,50)			4,60	16,1 (0,22)			6,00	16,9 (0,33)		

On the penetrogram graph (Fig. 6b), it is also presented the average of all 14 Panda 3® tests carried out close to each CPT (green line). A good agreement is observed between the cone resistance q_c average with CPT and these obtained by mean of Panda 3® (q_d) (Fig. 6b).

Although the MASW2D profiles in Fig. 6a show a spatial homogeneity, it is not observed on the CPTs and Panda penetrograms. In fact, all penetration tests shown an important heterogeneity of cone resistance in depth and space. This higher resolution with Panda 3® measurements is visible when we compare shear wave velocities between the three methods in Table 1. Panda 3® shear wave velocity averages are higher than with MASW and CPT (Jamiolkowski correlation [7] Eq (3) chosen, appropriate to sandy embankment), for the three layers. Moreover, the Panda 3® standard deviations on the shear wave velocities are higher than with the other methods, allowing to see every heterogeneity of soils. Also the Panda 3® method is a direct measurement method of a wave velocity. The MASW method is inclined towards to spread measurements and the CPT method derives from a correlation.

A summary of all the geotechnical results (q_d, q_c, E_M, p_{LM}, ρ, Vs) is given in Table 1, with averages and standard deviations for layers 1, 2 and 3 (< 6 m).

4. Results and discussion

4.1. Density profile

Soil density profiles were obtained by two methods, namely:

- CPT method
- Panda penetrometer method.

For the CPT method, the soil bulk density in place was calculated for each borehole from the correlation proposed by Robertson [43], i. e. Eq. (11) :

$$\gamma/\gamma_w = \frac{1}{2{,}65}\left[0{,}27\log R_f + 0{,}36\log\left(q_t/p_a\right) + 1{,}236\right]G_s \quad (11)$$

In the case of Panda test, the density was obtained from the correlations available in the device's database. For sands, the density is calculated from dynamic cone resistance q_d according to Eq. (12):

$$\gamma = A * \ln(qd) + B \quad (12)$$

With A and B the regression coefficients whose value for shall sands are about 0.97 and 15.81 respectively.

In this way, a very good agreement of both estimations is observed. The CPTs test were analysed from raw data while Panda test were analysed from regularized windows data (smoothed and averaged every 300 mm).

The bulk density profiles obtained are shown in Fig. 7, and the results show that the estimates made using the two methods correspond well to each other. The values retained for each layer are presented in Table. 1.

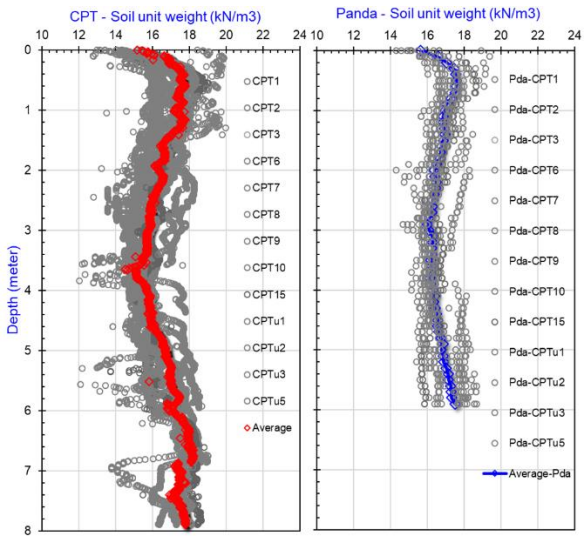

Figure 7. Experimental campaign on Sète Site. Unit weight density of silty sand embankment estimated by (a) CPT method and (b) Panda test density database.

4.2. Seismic / CPT Correlation / Panda 3® shear wave velocity

Shear wave velocity profiles are obtained by three different means:

- MASW in Fig. 8a
- CPT (literature correlations) in Fig. 8b and 8c
- Panda 3® method through analysing on each blow and polar shock approach

Panda tests were analysed from regularized windows data (smoothed and averaged every 300 mm). Also the average of the shear wave velocities of all Panda tests is represented in red.

We considered the groundwater table depth at 2.40m for the analysis.

For the groundwater table effects on shear wave velocity deduced from Panda3®, in wave measurement by means of polar shock method, measurement is made during the first milliseconds of shock, when the inertial forces and acceleration are greatest. It should also be noted that the measurement made corresponds to the compression velocity waves - as shown by [23], [34], [37], [38] – and shear wave velocity are deduced from plastic theory and Poisson coefficient.

Before 2.40 m, Poisson ratio is estimated at 0.33 and at 0.45 beyond in order to take into account the effect of the groundwater table on of the wave velocity, which would have increased under the groundwater table because of the increase of the compression wave velocity.

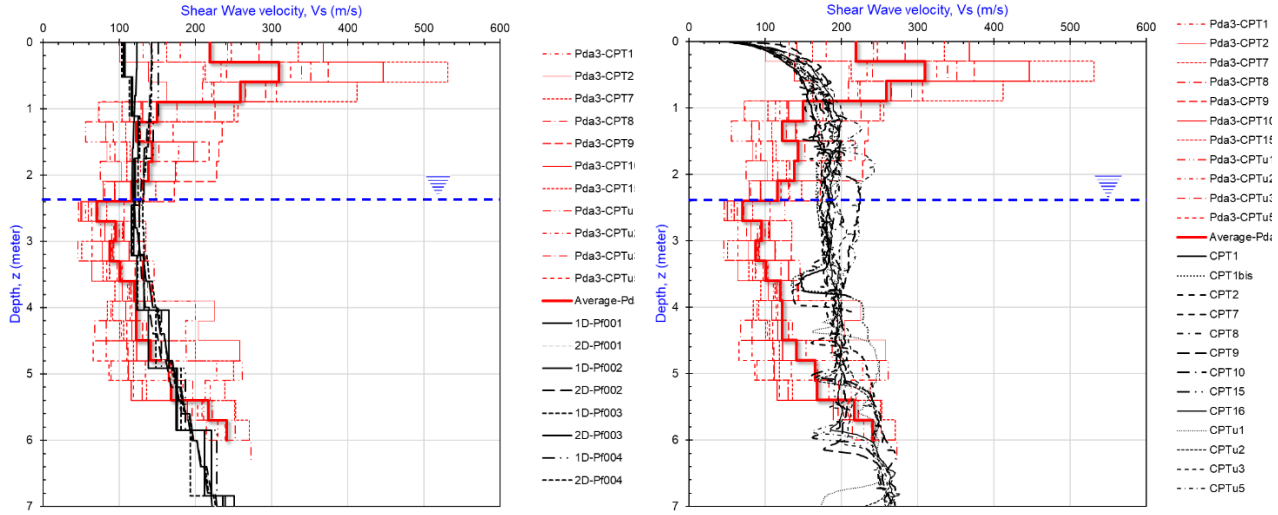

(a) MASW

(b) CPT-Jamiolkowski

(c) CPT-Robertson

Figure 8. Experimental campaign on Sète site. Comparison of all shear wave velocity profiles obtained by means MASW, CPT and Panda 3® tests. (a) Comparison of MASW and Panda3® Profiles and (b) CPTs and Panda3® profiles (Jamiolkowski) and (c) with CPT Robertson correlation.

For the first layer (0 – 1.80m), Panda tests show a better resolution for the high compacity of this layer, with a shear wave velocity higher than the MASW and CPT velocities. In the second layer, especially between 1.80 to 2.60 meters depth, a very good agreement is observed with both Panda 3 and MASW method and Robertson CPT correlation. Values with Jamiolkowski CPT correlation are higher than Panda 3 values.

Beyond 2.60 meters depth (under the groundwater table) a good agreement is observed with both Panda 3 and MASW method and Robertson CPT correlation. With Jamiolkowski CPT correlation, values remain higher than with Panda 3 from 2.60 to 5m, showing differences that can occur between correlations based on different contexts.

The observed differences, especially the visibility of heterogeneity with Panda 3, highlight either the limitations or the contribution of the measurements made with this new measurement technique. These differences can be explained by:

- Vertical and spatial variability of soil conditions and in consequence of mechanical parameters;
- Skin friction affecting penetrometer measurement,
- Panda3® measurement variability and influence of the water table.

In the case of skin friction, it has been verified during the accomplishment of each test the absence of torque. This was measured with a digital torque device every 1 meter depth.

If skin friction would occur, it has been demonstrated that it can be identified and corrected accurately by means of signal processing analysis methods developed for pile dynamic loading tests [31], [44].

Furthermore, spatial variability of soil that constitutes the backfill is sometimes significant (see Fig. 5b, Fig. 6, Fig. 7 and Fig. 8). This can be observed from CPT as well as Panda3® cone resistance measurements. Both tests are very sensitive to the vertical variability of soil conditions, and therefore allow it to be clearly identified. In contrast, MASW shear wave velocity deduced *Vs* measurements are much less sensitive to vertical variation. MASW tends then to homogenize *Vs* measurements in both vertical and horizontal directions. In addition, MASW measurements are obtained from inversion methods that require an initial terrain model. Although the results obtained are quite accurate at depth, on shallow surface their interpretation requires caution and some skills in signal processing. However, the order of magnitude of this type of measurement is often correct.

However, more detailed studies need to be carried out. It would be interesting to compare the values from Panda 3® with those obtained from seismic refraction, cross-hole or down-hole test.

5. Conclusions and perspectives

In this paper, we presented the lightweight dynamic cone penetration test Panda3®. The exploitation of Panda3®'s signals provides us many information not only on dynamic tip resistance but also on additional mechanical parameters involved during the driving of the tip, especially the tip's load displacement curve. The aim of this paper was to confirm the good agreement between soil shear wave velocity obtained through Panda 3® test and those obtained with CPT and MASW.

In the results of the last experimental campaign, a good agreement has been observed between the Panda 3® shear wave velocity and shear wave velocities obtained with traditional investigations. A higher precision in measurements has been observed with the Panda 3® method in comparison with MASW and CPT method. It is a direct measurement of soil characteristics. However, this method has a limited investigation depth. For example, this technique can be used as a complement with geophysical methods as MASW2D to define geotechnical model and/or to identify precisely soils which could be sensible to dynamic stresses (liquefaction) at the surface. It is also a fast and with a very low-cost technique to characterize surface soils. A coupling between Panda 3® method and other geophysical investigation methods could be a good alternative to the Cross-Hole method, which remains the principal method to determine a shear wave velocity for seismic classification or to characterize liquefaction potential until 30m depth, but also a long and expensive technique.

With the Grizzly-EV tests, it will be possible to obtain the same results with the same principle but with a deeper characterisation.

Acknowledgement

The project presented in this paper is supported by the Industrial Port of Sète, which allowed us to access to the site for our experimental campaigns.

6. References

[1] American Society for Testing & Mater, "Standard test methods for felt," pp. 1–10, 1987.

[2] C. B. Park, R. D. Miller, and J. Xia, "Multichannel analysis of surface waves," *Geophysics*, vol. 64, no. 3, pp. 800–808, 1999.

[3] J. Ameratunga, N. Sivakugan, and B. M. Das, *Correlations of Soil and Rock Properties in Geotechnical Engineering*. 2016.

[4] P. W. Mayne, "Stress-strain-strength-flow parameters from enhanced in situ tests . International conference on in situ measurement of soil properties & case histories," no. June 2018, 2001.

[5] P. W. Mayne, "In-situ test calibrations for evaluating soil parameters," *Characterisation Eng. Prop. Nat. Soils*, vol. 3–4, no. July, pp. 1601–1652, 2007.

[6] E. Flavigny, "Caractéristiques dynamiques des sols et reconnaissances," 2012.

[7] M. Jamiolkowski, D. C. F. Lo Presti, and M. Manassero, "Evaluation of relative density and shear strength of sands from CPT and DMT," *Geotech. Spec. Publ.*, vol. 40659, no. 119, pp. 201–238, 2003.

[8] R. D. Andrus, N. P. Mohanan, P. Piratheepan, B. S. Ellis, and T. L. Holzer, "Predicting shear-wave velocity from cone penetration resistance," *Proc. 4th Int. Conf. Earthq. Geotech. Eng.*, no. 1454, p. 12, 2007.

[9] P. K. Robertson, "Interpretation of cone penetration tests - a unified approach," *Can. Geotech. J.*, vol. 46, pp. 1337–1355, 2009.

[10] AFNOR, "Eurocodes 8 - Calcul des structures pour leur résistance aux séismes – Partie 1 : règles générales, actions

sismiques et règles pour les bâtiments," 2005.

[11] BRGM, "Cartographie automatique des classes de sol à l'échelle régionale à partir d'un modèle numérique de terrain ou de surface," 2010.

[12] D. M. Boore, "Estimating $\bar{V}s(30)$ (or NEHRP site classes) from shallow velocity models (depths < 30 m)," *Bull. Seismol. Soc. Am.*, vol. 94, no. 2, pp. 591–597, 2004.

[13] B. R. D. Andrus, A. Member, and K. H. S. Ii, "Liquefaction resistance of soils from shear-wave velocity," *J. Geotech. Geoenviron. Eng.*, vol. 126, no. November, pp. 1015–1025, 2000.

[14] R. Gourvès, "The Panda ultralight dynamic penetrometer." 1995.

[15] M.-A. Benz Navarrete, "Mesures dynamiques lors du battage du pénétromètre PANDA 2," Blaise Pascal Clermont Ferrand II, 2009.

[16] M. A. Benz Navarrete, E. Escobar, R. Gourvès, Y. Haddani, P. Breul, and C. Bacconnet, "Mesures dynamiques lors du battage pénétromètrique – Détermination de la courbe charge-enfoncement dynamique en pointe," in *18th International Conference on Soil Mechanics and Geotechnical Engineering, Paris 2013 Mesures*, 2013, no. 1, pp. 1–4.

[17] E. Escobar, "Mise au point et exploitation d'une nouvelle technique pour la reconnaisance des sols : le PANDA 3," 2015.

[18] J. C. Barré de Saint-Venant, "Mémoire sur le choc longitudinal de deux barres élastiques de grosseurs et de matières semblables ou différentes, et sur la proportion de leur force vive qui est perdue pour la translation ultérieure; et généralement sur le mouvement longitudinal d'un sys," *J. des mathémathiques pures appliquées*, vol. 4, pp. 27–74, 1898.

[19] S. Timoshenko and J. N Goodier, "The Theory of Elasticity," *SERBIULA (sistema Libr. 2.0)*, vol. 1, 1951.

[20] M. B. Abbott, "An Introduction to the Method of Characteristics," in *Finite Difference Methods in Financial Engineering: A Partial Differential Equation Approach*, American E., Thames and Hudson, Ed. New York: Cambridge University Press:, 1966, pp. 47–59.

[21] P. Middendorp and V. Weele, "Application of characteristic stress wave method in offshore practice," in *Proc. 3rd Int. Conf. on Numer. Methods in Offshore Piling*, 1986, pp. 6–18.

[22] M. N. Bussac, P. Collet, G. Gary, and R. Othman, "An optimisation method for separating and rebuilding one-dimensional dispersive waves from multi-point measurements. Application to elastic or viscoelastic bars," *J. Mech. Phys. Solids*, vol. 50, no. 2, pp. 321–349, 2002.

[23] A. Lodygowski, Tomasz, Rusinek, *Constitutive Relations under Impact Loadings*, CISM Inter. Springer, 2014.

[24] B. Lundberg, J. Carlsson, and K. G. Sundin, "Analysis of elastic waves in non-uniform rods from two-point strain measurement," *J. Sound Vib.*, vol. 137, no. 3, pp. 483–493, 1990.

[25] D. T. Casem, W. Fourney, and P. Chang, "Wave separation in viscoelastic pressure bar using single point measurements of strain and velocity," *Polym. Test.*, vol. 22, pp. 155–164, 2003.

[26] L. G. Karlsson, B. Lundberg, and K. G. Sundin, "Experimental study of a percussive process for rock fragmentation," *Int. J. Rock Mech. Min. Sci.*, vol. 26, no. 1, pp. 45–50, 1989.

[27] H. Zhao and G. Gary, "A new method for the separation of waves. Application to the SHPB technique for an unlimited duration of measurement," *J. Mech. Phys. Solids*, vol. 45, pp. 1185–1202, 1997.

[28] J. Carlsson, K. G. Sundin, and B. Lundberg, "A method for determination of in-hole dynamic force-penetration data from two-point strain measurement on a percussive drill rod," *Int. J. Rock Mech. Min. Sci.*, vol. 27, no. 6, pp. 553–558, 1990.

[29] E. A. L. Smith, "Pile driving analysis by the wave equation," *J. Soil Mech. Found. ASCE*, vol. 86, pp. 35–61, 1960.

[30] G. G. Goble, F. Rausche, and G. E. Linkins, "Analysis of Pile Driving - a State-of-the-Art.," *IEEE Journal of Solid-State Circuits*. pp. 131–161, 1981.

[31] R. Frank, M. Fred, and G. G. G., "Soil Resistance Predictions From Pile Dynamics," *Current Practices and Future Trends in Deep Foundations*. pp. 418–440, 18-Apr-2019.

[32] P. Reiffsteck, C. Bacconnet, R. Gourvès, E. Goddé, and H. van de Graaf, "Determination of elastic modulus from stress controlled cone penetration test," in *3rd International conference on Site Characterization*, 2008, no. April, pp. 1135–1138.

[33] E. Escobar, M. A. Benz Navarrete, R. Gourvès, Y. Haddani, P. Breul, and B. Chevalier, "Dynamic Characterization of the Supporting Layers in Railway Tracks Using the Dynamic Penetrometer Panda 3®," in *Procedia Engineering*, 2016, vol. 143, pp. 1024–1033.

[34] M. A. Benz Navarrete, E. Escobar, Y. Haddani, R. Gourves, S. Costa D'Aguiar, and N. Calon, "Determination of soil dynamic parameters by the Panda 3®: Railways platform case," in *Civil-Comp Proceedings*, 2014, vol. 104, pp. 1–15.

[35] E. Escobar, M. A. Benz Navarrete, Y. Haddani, F. Lamas-Lopez, N. Calon, and S. Costa D'Aguiar, "Reconnaissance Dynamique Des Sites Ferroviaires a L ' Aide Du Penetrometre Panda 3 ®," in *Journées Nationales de Géotechnique et de Géologie de l'Ingénieur JNGG2014*, 2014, p. 11.

[36] G. Aussedat, "Sollicitations rapides des sols," 1970.

[37] J. Meunier, "Contribution à l'étude des ondes et des ondes de choc dans les sols," Grenoble, 1974.

[38] J. F. Semblat, M. P. Luong, and G. Gary, "3D-Hopkinson bar: New experiments for dynamic testing on soils," *Soils Found.*, vol. 39, no. 1, pp. 1–10, 1999.

[39] R. H. Tatham, "Vp/Vs and lithology," *Geophysics*, vol. 47, no. 3, pp. 336–344, 1982.

[40] L. V. Socco and C. Strobbia, "Surface-wave method for near-surface characterization: a tutorial," *Near Surf. Geophys.*, vol. 2, no. 4, pp. 165–185, 2004.

[41] E. J. Escobar Valencia, M. A. Benz Navarrete, R. Gourvès, P. Breul, and B. Chevalier, "In-situ determination of soil deformation modulus and the wave velocity parameters using the Panda 3®," in *5th Geotechnical and Geophysical Site Characterisation, ISC5*, 2016, pp. 279–284.

[42] E. J. Escobar Valencia, "Mise au point et exploitation d'une nouvelle technique pour la reconnaisance des sols : le PANDA 3," University Blaise Pascal, Clermont II, 2015.

[43] P. K. Robertson and K. L. Cabal, "Estimating soil unit weight from CPT," *2nd Int. Symp. Cone Penetration Test.*, no. May, p. 8 p., 2010.

[44] M. H. Hussein and G. G. Goble, "A Brief History of the Application of Stress-Wave Theory to Piles," in *Contributions in Honor of George G. Gobel*, 2004, pp. 186–201.